DGPF PROJECT: EVALUATION OF DIGITAL PHOTOGRAMMETRIC AERIAL BASED IMAGING SYSTEMS – OVERVIEW AND RESULTS FROM THE PILOT CENTRE

Michael Cramer & Norbert Haala

Institut for Photogrammetry (ifp), Universitaet Stuttgart, Geschwister-Scholl-Str. 24D, D-70174 Stuttgart, Germany
(michael.cramer, norbert.haala) @ifp.uni-stuttgart.de

KEY WORDS: Digital camera, empirical accuracy, geometric performance, automated DSM generation

ABSTRACT:

Within the paper results of a test on the evaluation of new photogrammetric digital airborne camera systems are presented. This project was initiated by the German society of Photogrammetry, Remote Sensing and Geoinformation (DGPF). Based on data flown in a well controlled site a test bed for the comprehensive performance analyse of digital camera systems was defined. Data collection was realised for 12 different photogrammetric systems and a network of more than 25 participating institutions was established. The main topics of the evaluation phase are the analysis of geometric accuracy and sensor calibration, the radiometric performance including on-site radiometric calibration and multi-spectral land classifications, the performance of photogrammetric DSM generation and the potential of manual stereo plotting from digital images. These topics are covered by four working groups. Within this paper results obtained at the Institute for Photogrammetry (ifp), Universitaet Stuttgart will be presented. The ifp served as the pilot centre of the test and additionally concentrated on the investigation of camera geometry and the image based generation of height data.

1. INTRODUCTION

Triggered by the dynamic development of digital airborne photogrammetric cameras the testing and independent evaluation of these systems is an ongoing issue. Such tests are frequently driven by individual institutions or even national or international organizations. Primarily they help to gain a knowledge base in digital camera performance which is then for example used for decision-making when changing from analogue to digital sensor flights. Despite the fact, that some national mapping agencies decided to switch to digital image recording and abandon their old analogue cameras and film development equipment, comprehensive testing of the latest generation digital sensor systems including the quality analysis of sensor products (i.e. covering the whole process line) was typically not considered so far (see e.g. [Passini & Jacobsen, 2008], [Cramer, 2007]). This was the motivation of the German society of Photogrammetry, Remote Sensing and Geoinformation (DGPF) to define a test bed to comprehensively analyse the performance of photogrammetric digital airborne camera systems. Focus is laid on airborne and large format photogrammetric sensor system. The test is not limited to sensor performance but also investigates on the software processing chain which is another important component when photogrammtric products are of interest. In order to allow for a comprehensive analysis, the data had to be captured in similar test flight conditions and controlled environments. For this purpose comprehensive flight campaigns were realized in the Vaihingen/Enz photogrammetric test site, established and maintained by the Institut for Photogrammetrie (ifp), Universitaet Stuttgart. During the camera test, the ifp served as pilot centre during data collection and preparation and also managed the data distribution to the various participants.

The data is made available for all types of institutions ranging from science, mapping authorities, photogrammetric companies and sensor providers. Meanwhile, more than 25 different institutions have signed the project agreement where the common topics of analysis and a corresponding schedule were fixed. Meanwhile, almost all participants requested and received the respective data sets. One of the key ideas of the project is to form a network of expertise from these institutions. In order to structure this cooperation during data evaluation, four working groups were established which are focusing on the topics geometry, radiometry, digital surface models and stereoplotting. First results of the participating groups were presented at the annual meeting of the German Society of Photogrammetry, Remote Sensing and Geoinformation (DGPF) in Jena in March, 2009. Additionally a project web site (in German) is available to document project progress and disseminate most recent information [DGPF, 2009].

The **main objective of this DGPF test is not to directly compare performance of the different sensors but to evaluate the sensor specific strengths and maybe weaknesses**, which are of relevance when later choosing a sensor for specific applications. Still, all findings obtained from this test always are based on the results of the DGPF test flights only and have to be confirmed from other tests.

After a presentation of the data collection phase of the test (airborne sensors and ground reference data) in the following section, this paper focuses on the ongoing investigations at the pilot centre in Stuttgart. The evaluations concentrate on the issues geometric accuracy and reference orientations for camera systems as presented in section 3 and the performance of photogrammetric DSM generation using these systems, which is described in section 4. During these tests the frame based camera systems DMC, Ultracam-X and quattro DigiCAM were investigated, in order to compare their performance to the performance from classical analogue cameras (RMK-Top15).

2. DATA COLLECTION

The data collection was realised in the photogrammetric test site Vaihingen/Enz close to Stuttgart, which is already known from other performance tests. It comprises close to 200 signalized and coordinated reference ground points distributed in a 7.4 x 4.7 km² area.

2.1 Flight campaigns

The imaging data was flown at 6 different flight days during a 10 weeks time window starting beginning of July till mid of September 2008. Originally a much shorter 2 weeks time period was planned for data acquisition, which could not be realized due to weather conditions. The different flight campaigns from summer 2008 are listed in Table 1. Most sensors were flown in two different flying heights, resulting in two blocks with previously defined different ground sampling distances (GSD), namely GSD 20cm and GSD 8cm (nominal values). Additional flights were done with a Leica ALS 50 LiDAR and the AISA+ and ROSIS hyperspectral scanner in order to later use this data as reference for the photogrammetrically derived surface models and multi-spectral land cover classification.

System	Vendor	System flyer	Days of flight
DMC	Intergraph/ZI	RWE Power	24.07.08 06.08.08
ADS 40, 2nd	Leica Geosyst.	Leica Geosyst.	06.08.08
JAS-150	Jenaoptronik	RWE Power	09.09.08
Ultracam-X	Vexcel Imaging Graz	bsf Swissphoto	11.09.08
RMK-Top15	Intergraph/ZI	RWE Power	24.07.08 06.08.08
Quattro DigiCAM	IGI	Geoplana	06.08.08
AIC-x1	Rolleimetric	Alpha Luftb.	11.09.08
AIC-x4	Rolleimetric	Vulcan Air	19.09.08
DLR 3K-camera	DLR Munich	DLR Munich	15.07.08
AISA+ hyper-spectral	specim FH Anhalt	RWE Power	02.07.08
ROSIS hyper-spectral	DLR München	DLR Munich	15.07.08
ALS 50 LiDAR	Leica Geosyst.	Leica Geosyst.	21.08.08

Table 1: Participating sensor systems and flying companies

The GSD 20cm blocks were flown with 60%/60% overlap conditions, whereas for the GSD 8cm block a higher forward overlap of 80% was aspired. Due to the fixed test site extensions and different sensor formats slight modifications of the block geometry were necessary which potentially influences the later comparison of sensor performances. Additionally not all cameras finally fulfilled these overlap requirements. Some of the sensors were only flown in one flying height (namely the AIC-x1 and 3K-camera flights) other data sets were influenced by technical problems.

Variations in weather conditions also have to be considered especially when looking for the radiometric sensor performance. Almost all flights were affected by clouds. Additionally, due to the test period of more than 2 months, there were significant changes in vegetation and sun angle. Some of the flights were done quite early in the morning, others were flown around noontime.

In all cases the sensor flight data was delivered through the system manufacturer itself to the project pilot centre. All manufacturers had access to 19 ground control points to check that their data sets are consistent and comparable to other flights. This was done before the data was sent to the pilot centre for further dissemination. Obviously some of the sensor providers used the reference points to already go into deeper analysis of the sensor performance. Thus, the finally delivered data sets not in all cases may fully reflect the standard quality (status of pre-processing) of a data set which is obtained in a typical operational survey mission scenario.

2.2 Reference data from the ground

Spectrometer measurements were done on the ground, parallel to the sensor flights to get ground references for the later atmospheric corrections and sensor calibrations. This was supported by sun-photometer measurements, which determine the optical depth of the atmosphere, and thus also reflect weather and cloud conditions during the flights. Bidirectional reflectance values were acquired with a special BRDF measurement set-up. Spectrometer measurements were done for artificial and natural targets, but only a few natural objects like asphalt or grass surfaces have been measured but not consistently for all flight campaigns. Figure 1 shows major parts of the radiometric test range and ground team members during reference measurements parallel to the sensor flights. The artificial colour targets and different resolution test targets (Siemens star) can be seen. It has to be mentioned that the relatively small colour targets (size 2x2m²) typically were only sufficient for the GSD 8cm flights, especially when the original colour information is acquired with less spatial resolution compared to pan-chromatic images. This is the case for the DMC and Ultracam-X frame based sensor systems, where coloured large format images are obtained from pan-sharpening. For radiometric analysis the original colour information before pan-sharpening is of main interest. The remaining frame sensors AIC, quattro DigiCAM and 3K-Camera use the Bayer pattern for colour generation.

Figure 1: Ground teams performing reference measurements in radiometric test field

The spectrometer reference measurements are basis for an on-site absolute radiometric sensor calibration (so-called vicarious calibration). Such calibration originally was planned. First

investigations using the known ATCOR program [Richter 2009] for atmospheric correction were already done. Unfortunately, this analysis finally showed that the spectral behaviour of the almost exclusively measured artificial colour targets is quite different from natural targets. Figure 1 already shows their strong directional reflectance behaviour which is not expected for natural targets. Additional neighbouring effects from the surrounding grass due to the limited size of the targets finally prevent the aspired absolute radiometric calibration of the airborne sensors [Schönermark et al., 2009].

To complete the reference data for comprehensive radiometric performance analysis, extensive field-walkings were done for documentation of different land use. This especially was quite time consuming, because surveys had to be repeated several times in order to document the changes in land coverage due to the quite long flight interval [Klonus et al., 2009].

3. GEOMETRIC ACCURACY ANALYSIS

As already mentioned the project is structured in four different working topics. Besides analysis of the geometric and radiometric sensor performance, the evaluation of sensor products like image based automatic surface models or manual stereoplotting is of concern. This not only reflects the quality of the individual sensor but also includes the corresponding software processing chain. The process of product generation and to a certain extent already the radiometric performance investigations (i.e. BRDF analysis) rely on results from geometric data processing. The exterior orientation is essential information for the product generation process. It is obtained from aerial triangulation, which is deeply analysed from the experts in the geometrical aspects group. In order to avoid delays in the evaluation of automatic surface models and stereo plotting, it was decided that a nominal set of exterior orientation elements will prepared by pilot centre. For later comparison all products are based on these nominal exterior orientation elements. These nominal values not necessarily represent the most optimal result for sensor orientation – this will be one of the results of the geometry group – but still should be accurate enough for use in the working packages automated DSM generation and stereoplotting. Due to limitations in time the sensor orientation at pilot centre was first done for the digital frame based sensor systems DMC, Ultracam-X and quattro DigiCAM, as well as for the digitized RMK-Top15 image blocks.

3.1 Nominal exterior orientation values

Within aerial triangulation the use of additional parameters is necessary to overcome remaining systematic effects, i.e. to adapt the mathematical model to the physical process of image formation. Earlier investigations on self-calibrating bundle adjustment already underlined the sometimes significant increase in object point quality when using standard or specially designed additional parameter models [Cramer 2007, Jacobsen ???], especially when dealing with image data from digital cameras. The problem now is to apply the corrections from additional self-calibration for later processing steps also. This especially is of concern, if different software products are used for the sensor orientation and later production. Typically most of the aerial triangulation software packages derive correction grids from the additional parameter sets, which then are considered in the following processing steps. However, since there is no standard for correction grids available, the transfer of correction grids between software chains from different providers is at least error-prone.

In order to prevent this problem, but still use most of the information from additional parameters, a so-called absolute orientation was performed for the determination of the nominal exterior orientations. This is a two-step process. In the first part a self-calibrating aerial triangulation is done, based on all available signalized object points as control points. In our case the 110 control points and additional 77 check points are available. All of them were used as control points here. In our case no additional observations from GPS or GPS/inertial have been introduced. The standard 44 parameter model proposed by Grün was used for self-calibration. Only the significant parameters were estimated. Thus this first part determines self-calibration parameters and adjusted object coordinates.

The second step, which is now called absolute orientation[1] step, is based on the object coordinates only, including the already known signalized points and the previously determined object points from self-calibrating AT as fixed observations. All these points are used as fixed observations, thus the elements of exterior orientations are the only unknowns to be determined within this bundle adjustment. Due to the fixing of all degrees of freedom except the orientation elements, main parts of the effect from self-calibration is projected into the orientation elements. These orientation parameters are then used as nominal values for the DSM generation and stereoplotting.

Image block	σ0	# obj. points	redun-dancy	# max. rays	# sign par.	max. corr. [µm]	
						x	y
RMK GSD 8cm	4.09	2675	20011	13	44	4.0	4.1
RMK GSD 20cm	4.34	1970	20495	16	17	4.9	4.2
DMC GSD 8cm	1.49	9651	80371	13	44	2.2	1.3
DMC GSD 20cm	1.98	5432	49366	12	10	5.3	3.5
UC-X GSD 8cm	0.95	6049	109906	28	6	0.7	0.9
UC-X GSD 20cm	1.07	4729	43932	12	4	0.4	1.1
Quattro DigiCAM GSD 8cm	0.99	30872	629043	33	3(1)	1.1	0.9
					9(2)	1.5	2.3
					3(3)	0.9	1.4
					4(4)	1.8	1.5
Quattro DigiCAM GSD 20cm	1.28	20501	192240	18	3(1)	1.0	1.1
					10 (2)	1.8	2.4
					4(3)	0.9	1.0
					6(4)	2.1	1.2

Table 2: Self-calibrating AT (44 parameters) using all GCPs

Table 2 summarizes results from the first step, the self-calibrating AT using the significant terms of the 44 additional parameter model for the three digital frame sensors in comparison to the RMK-Top15 blocks. Since all object points are used as control points no external accuracy estimation is

[1] The term absolute orientation in its narrower sense is related to relatively oriented stereo models where arbitrarily model coordinates are brought to the desired object coordinate frame. This is done by spatial similarity transformation (scaling, levelling, and orientation) based on ground control points [Kraus, 2007].

possible. Thus the table only reflects internal accuracy and some basic information on the block geometry itself. The processing was done using the PAT-B software. For automatic tie and manual control point measurements the Match-AT software was used. Measurements were done in the 16bit RGB images for DMC and quattro DigiCAM and in 8bit PAN images for Ultracam-X. The coloured analogue RMK-Top images (CN film for GSD 8cm and CIR for GSD 20cm block) were scanned with 14µm resolution and 3x8bit/pix.

The given values for redundancy, maximum number of image rays for individual object points and the overall number of object points within each block clearly illustrate the different block geometries. This always has to be considered when comparing results from different sensors. The GSD 8cm blocks were flown with 80%/60% overlap for DigiCAM and Ultracam-X but with 60%/60% for DMC. The GSD 20cm blocks were flown with 60%/60% overlap for all digital systems. In case of quattro DigiCAM the overlap is related to the area covered by the four camera heads of one exposure station, although the four images are kept as individual and not merged to one large format virtual image. The table also shows that typically more homologous points are delivered from image matching for digital images. This is due to the better radiometry (signal-to-noise ratio) compared to the scanned analogue RMK images. Thus the number of object points is significantly less for the RMK-Top15 blocks. The quattro DigiCAM blocks have the largest number of block points and highest redundancy. They also obtain highest values for the maximum number of image rays per single point. This is also due to the significant higher number of images per block and the overlap between the 4 images of one exposure time.

The obtained σ0 values are quite similar for the digital systems. The value for RMK-Top15 is about 2-4 times worse which should be expected due to the analogue data acquisition. Additionally the redundancy of the adjustment also has influence on the σ0 values.

The three last columns of Table 2 are dedicated to the influence of the additional parameters introduced for self-calibration. For the quattro DigiCAM a separate set of 44 parameters was introduced for each camera head. Only the significant parameters are finally considered. Typically only a smaller sub-set of the full 44 parameter set is finally estimated as significant parameters. Only for the GSD 8cm blocks of RMK and DMC all 44 parameters are estimated as significant values. Determinability of significance is always due to the specific block geometry (i.e. overlap conditions, number distribution of control points). Since the RMK and DMC GSD 8cm are flown with 60%/60% overlap only, their geometry is different to the remaining two other GSD 8cm blocks. The maximum correction from significant additional parameters in image space is obtained from 5 x 5 regularly distributed grid points. All these corrections are within sub-pixel range. Only the maximum value in x and y component is given in the table. Smaller differences are visible comparing the larger corrections in RMK-Top15 images to the digital cameras. For DMC larger influences are seen in the GSD 20m block compared to the GSD 8cm block. This might be explained by the collocation grid correction which was applied by Intergraph in the DMC GSD 8cm images but not for the GSD 20cm block.

3.2 Absolute geometric accuracy

The geometrical accuracy investigations presented so far did not allow for absolute accuracy checks, because no independent check points were available. Till now, all available object points were introduced as control points. Within this section the number of control points was reduced to 70 GCPs for the GSD 20cm blocks and 60 GCPs for the GSD 8cm flights. Thus, the remaining signalized object points were used as independent check points, resulting in about 115 and 50 check points for GSD 20cm and GSD 8cm respectively. Compared to the size of the block, this still is a high number of control points. Control points are available at the border of each block and in 5 additional control point chains, perpendicular to the main flight direction. Again no additional observations from GPS/inertial sensors were introduced. Image coordinates used for these bundle adjustments already have been corrected by the previously estimated influence of self-calibration, based on all available control points. Thus no additional self-calibration was considered here. Due to these two aspects, the following results may give a too optimistic estimation of the geometrical accuracy potential of the sensors. Such accuracy not necessarily could be expected for later operational (more realistic) sensor flights when less control points are used and larger blocks are flown. The following object point accuracy only might be achieved in optimal conditions.

Table 3 and Table 4 show the results from check point analysis separated for the GSD 20cm and GSD 8cm blocks. The empirical RMS values from check point differences and the theoretical accuracy (standard deviation STD) of object point determination from inversion of normal equations is given. Results from digital sensors are compared to the RMK-Top results. Nevertheless, when comparisons between systems are done the different flight and block conditions have to be taken into account as already mentioned.

Image block	# GCP / ChP	RMS [m]			STD [m]		
		ΔX	ΔY	ΔZ	σX	σY	σZ
RMK GSD 20cm	70 / 116	0,03	0,04	0,05	0,03	0,04	0,07
DMC GSD 20cm	70 / 114	0,03	0,04	0,08	0,02	0,02	0,06
UC-X GSD 20cm	70 / 112	0,03	0,03	0,07	0,02	0,02	0,06
DigiCAM GSD 20cm	70 / 116	0,04	0,05	0,09	0,02	0,03	0,09

Table 3: Empirical accuracy RMS and STD – GSD 20cm

Image block	# GCP / ChP	RMS [m]			STD [m]		
		ΔX	ΔY	ΔZ	σX	σY	σZ
RMK 74 photos	60 / 48	0,02	0,02	0,03	0,01	0,02	0,03
DMC 136 photos	60 / 47	0,02	0,02	0,04	0,01	0,01	0,02
UC-X 215 photos	60 / 50	0,01	0,02	0,04	0,01	0,01	0,02
DigiCAM 784 photos	60 / 50	0,02	0,02	0,03	0,01	0,01	0,02

Table 4: Empirical accuracy RMS and STD – GSD 8cm

The obtained accuracy from these adjustments is very similar for all sensor systems. The absolute accuracy RMS (horizontal component) is in the range of ¼ pix or better related to GSD for both flying heights. For the vertical component, an accuracy of ½ pix and better is obtained. When the empirical RMS values are compared to the estimated STD from error propagation,

good agreement can be seen for the vertical axis. In case of the horizontal components the theoretical accuracy higher compared to the RMS values (mostly close to factor 2). This may indicate small not completely modelled errors. In this case the accuracy of reference point determination (based on static GPS base line observations) also is of influence. Since the GPS reference coordinates are determined with an accuracy of 1cm for horizontal and 2cm for vertical coordinates, the accuracy of object points from bundle adjustment is already in the accuracy range of the reference points.

Obviously the 44 parameter model used to correct the image coordinates is of sufficient accuracy for all sensor systems. Since this self-calibration model is implemented in most of the bundle adjustment software it can be used for a pragmatic processing of digital image blocks. Still it has to be confirmed, whether this pragmatic approach is also valid for larger blocks from operational flights supported by GPS/inertial sensors. Other AT software suppliers have introduced and implemented new additional parameter models, which take care of the special digital sensor geometry. The project working group geometry will evaluate these new approaches against the traditional models.

4. IMAGE BASED 3D DATA COLLECTION

As it was already demonstrated by the results of the geometric accuracy analysis, one well known advantage of digital airborne cameras is the good signal-to-noise ratio and the high dynamic range of the collected imagery, which considerably improves the accuracy and reliability of automatic point transfer by image matching compared to scanned analogue images. Image matching is not only used as basic observation for bundle block adjustment, but is also the main prerequisite for 3D surface reconstruction. In addition to the improved matching accuracy, this process additional benefits from redundant information as it is provided from highly overlapping images, which are especially available for th e GSD 8cm flights in the test. In principle, such increased forward overlap can be collected at almost no additional costs if digital airborne cameras are used.

The use of automatic image matching for the generation of elevation data is well known for more than two decades. However, the improvements in the available quality of aerial imagery also resulted in a renaissance of software development. As an example, algorithms which fully exploit the potential of digital aerial cameras by extending the traditional stereo matching to a multiple image matching have been implemented just recently. Examples for such commercial software systems are Next Generation Automatic Terrain Extraction (NGATE) from BAE Sytems [DeVenecia et al., 2007] or MATCH-T DSM from INPHO GmbH [Lemaire, 2008] which is used for the investigations presented in this paper.

4.1 Generation and evaluation of 3D point clouds

Modern photogrammetric software systems optionally generate 3D point clouds as a result from multiple image matching. In addition to the traditional 2.5D raster representations of Digital Surface Models, such point clouds can for example be used during 3D object reconstruction in following processing steps. For our investigations point clouds are especially suitable since they allow for accuracy analyses of results from automatic image based 3D data collection while avoiding the influence of interpolation procedures. Firstly, the geometric accuracy of matched 3D points can be determined. Additionally, the density of the generated points indicates the quality of the matching process.

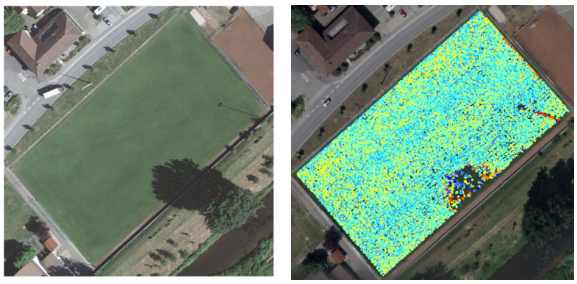

Figure 2: DMC image (left) and ortho image with color-coded point cloud overlaid (right)

Within our investigations 3D point clouds were computed and evaluated for the data from the frame based camera systems DMC, quattro DigiCAM, Ultracam-X and RMK-Top15. In order to evaluate the accuracy of the generated 3D point clouds by a relatively simple process, a test area at a planar sports field was defined. A DMC image of this field captured at GSD 8cm is depicted in Figure 2 (left). The result of the 3D point generation from this image block as overlaid to an ortho image is depicted in the right part of Figure 2. Within the area sports field a point density of 19.67 Pts/m^2 was generated. In order to evaluate the height accuracy of these points, an approximating plane was estimated. It resulted in a standard deviation of 9.7cm for the generated point measurement. As it is also indicated by the colour coded height of the 3D points, gross errors are available in the data set. These errors mainly occur at shadow areas, which in the example of Figure 2 result from a tree and a floodlight pole. In our investigations, stereo image pairs are processed, which either overlap along track or across track. While shadow movement is no problem for image matching if only data from one strip is used, problems might occur due to the increased time gap while combining image data from multiple strips. In such scenarios time dependent shadow movement can result in considerable errors of automatic point transfer, especially if high resolution images are used.

In order to allow for an objective comparison of image flights which were captured at different points of time, an elimination of these time dependent matching errors caused by shadowed areas is required. During our evaluation at the planar sports field, these gross errors were eliminated in a relatively simple two step procedure. First, the standard deviation was computed by estimating an approximating plane for all points as available from image matching. In a second step a threshold of $\pm 3\sigma$ was used to eliminate all points, which are potentially subjected to a gross error. For the example given in Figure 2 all points with a distance larger than ±3x9.7cm with respect to the approximating plane were eliminated. As it is also visible in the first row of Table 5, 1.3% of all points were eliminated as gross error, while as shown in the first column of the same row, the remaining filtered points had a standard deviation of 5.2cm.

In addition to the results for the flight GSD 8cm of the DMC camera Table 5 also shows the results for the remaining camera systems Ultracam-X, DigiCAM and RMK. The last row of this table additionally provides the results for the LiDAR data from the ALS 50 sensor for comparison. The results for the GSD 20cm imagery are presented in Table 6. The density and the percentage of eliminated measurements for the generated point

clouds are presented additionally in Figure 3. From top to bottom the respective results for DMC, Ultracam-X, DigiCAM and RMK are presented. The point distributions from the GSD 8cm blocks are given on the left, while the results for GSD 20cm are presented on the right. Points which were eliminated by the filter process are marked in light blue, while the remaining points are depicted in red. Similar to the right image of Figure 2, an ortho image is used as background.

Sensor	STD after filter [cm]	STD no filter [cm]	Elim.Pts [%]	Density Pts/m^2
DMC	5.2	9.7	1.3	19.67
Ultracam-X	6.8	8.0	0.4	19.04
DigiCAM	10.2	11.2	0.7	20.83
RMK	17.2	27.3	3.2	0.77
ALS 50	1.8	1.9	0.5	8.25

Table 5: Accuracy of 3D point clouds – GSD 8cm

Sensor	Stdv. after filter [cm]	Stdv. no filter [cm]	Elim.Pts [%]	Density Pts/m^2
DMC	17.2	25.4	1.1	2.71
Ultracam-X	22.6	34.2	0.4	1.62
DigiCAM	34.1	48.2	2.5	2.64
RMK	60.6	66.2	0.7	0.31

Table 6: Accuracy of 3D point clouds – GSD 20cm

During test data acquisition, the DMC and RMK images were recorded almost simultaneously at identical atmospheric and illumination conditions by using a double-hole aircraft. Thus, the advances of digital image acquisition for the image based generation of elevation data can be demonstrated very well from these data sets. This is clearly indicated by the much higher density of matched points from DMC images. Table 5 gives a value of about 20 pts/m² for the GSD 8cm DMC images, while matching of scanned RMK images gives less than 1 pt/m². Apparently, the higher radiometric quality of digital images obviously allows for much denser point matching while RMK-Top15 imagery is not suitable for the automatic derivation of high accurate surface models. Table 3 and Table 4 as well as Figure 3 document this supremacy for all digital camera systems, despite the fact, that the Ultracam-X and quattro DigiCAM images were captured at different points of time, which results in moderate differences in atmospheric conditions and illumination. Also changes in vegetation may have certain impact.

These differences have to be considered together with slight variations of the block geometry if the results for the digital camera systems are compared to each other. However, the advantage of point matching for the GSD 8cm blocks with 80%/60% overlap compared to the GSD 20cm blocks with 60%/60% overlap is striking for all digital camera systems. On average, a point density of about 20 pts/m² was reached using the GSD 8cm images from the digital camera systems. This value is even higher is even higher than the 8.25 pts/m², which were generated by the ALS 50 laser scanner at the sports field. However, the standard deviation for the LiDAR data is better than 2cm, almost without any gross errors, while an average of 7.4cm for the filtered points is achieved from image matching. Thus accuracy below 1 pixel GSD was achieved for the 8cm block. For the GSD 20cm this value is slightly worse with an average standard deviation of 24.6cm for the digital cameras. Compared to the 8cm GSD block, the average point density of 2.3 pts/m² is much lower. For this reason, especially height data as it can be provided from largely overlapping high resolution imagery like the GSD 8cm blocks seems to be at least comparable to 3D data from LiDAR measurement. Despite the fact that LiDAR still provides data of highest quality, a considerable number of applications is feasible based on height data from image matching, if digital airborne cameras are used.

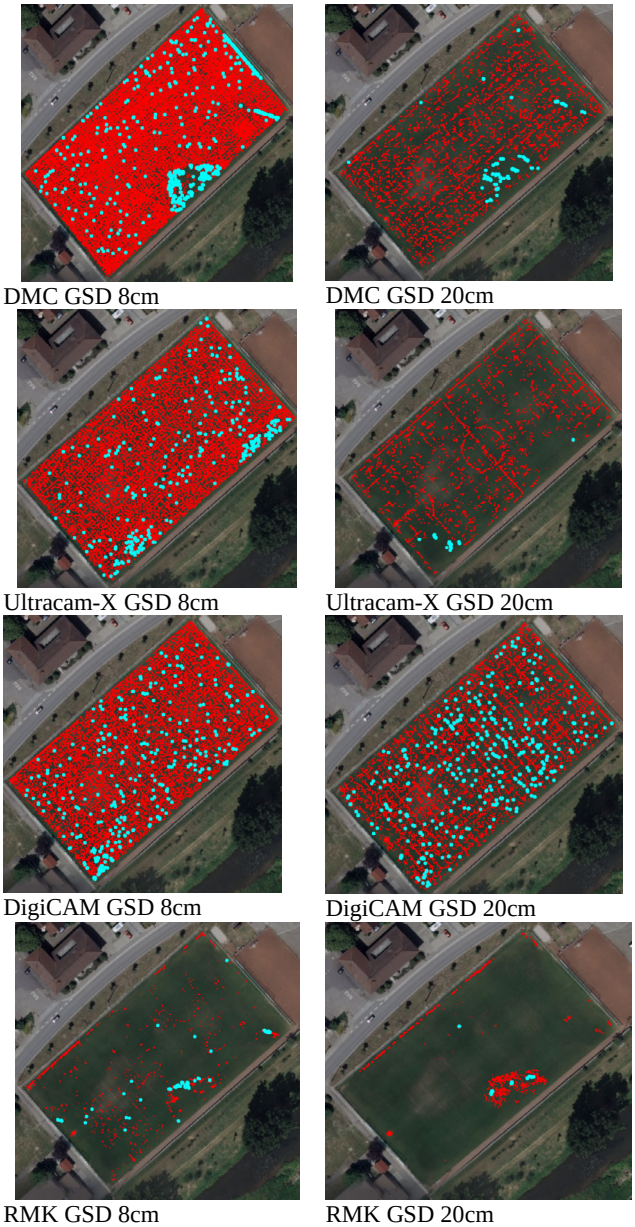

Figure 3: Point clouds from image matching, eliminated points marked in blue

4.2 Overall accuracy – height differences at signalised points.

The standard deviations which were presented in the previous section for the flat area of the sports field just give a value for the relative accuracy of point measurement. There, the point differences refer to the approximating plane estimated for the respective measurements. In order to enable an exterior quality check of image based elevation data, high accurate coordinates from the GPS measurements of the signalised control points in our test field were used. These points, where compared to DSM raster data as derived from the respective image blocks. In our investigations DSM raster of 25cm grid size were generated from GSD 8cm imagery, while the results from GSD 20cm blocks were used to generate a 50cm DSM raster.

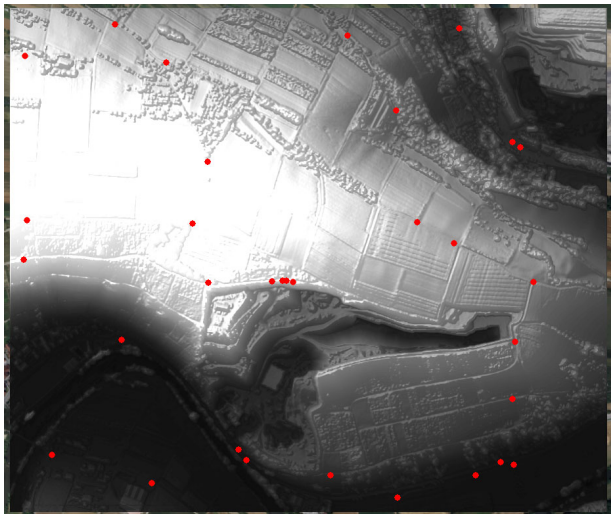

Figure 4: DSM with available control points

An example of such a DSM raster in combination with the signalised control points is depicted in Figure 4 .

	Sensor	RMS [cm]	Mean [cm]	Δ Max/Min [cm]	
GSD 8cm	DMC	3.3	2.0	7.4	-3.0
	Ultracam-X	3.0	0.4	5.3	-6.9
	DigiCAM	4.9	1.0	10.4	-7.6
GSD 20cm	DMC	12.8	7.0	19.6	-23.4
	DigiCAM	7.4	0.5	13.2	-15.3
	Ultracam-X	8.6	3.0	21.2	-11.7
	ALS 50	2.6	1.1	5.8	-5.3

Table 7: Computed differences at signalized GPS-points

Overall, 32 control points were available in the selected area. Table 7 gives the resulting RMS values from the differences of the DSM grids at these reference points. In order to limit the influence of coarse errors i.e. due to occlusions, always the point with maximum difference was eliminated before computation of the RMS value as well as the maximum and minimum and mean difference, which are also represented in Table 7. Using the remaining 31 control points on average an RMS of 3.7cm was obtained for the GSD 8cm images and 9.6cm RMS for the GSD 20cm imagery. The differences from the ALS 50 DSM of 2.6cm are almost in the range of the reference heights from GPS measurement.

Of course, the computed height differences are at the signalized points are not only influenced by the quality of the image matching process. In that scenario, there is a considerable impact of the geometric accuracy of the respective blocks, which were already investigated in the previous section.

5. CONCLUSION

Although the processing of the DGPF test flight data is still in an early phase the benefits of digital image recording for photogrammetric processing were proven impressively. Under optimal conditions the performance of 3D object point and elevation model generation is close to the quality of the reference data. It is not only the imaging sensor, the software chain and influences like environmental conditions during data acquisition increase in importance. Due to the relatively long test period of more than 2 months, these conditions were subjected to considerable change, which has to be considered if the results for the different camera systems are compared in detail.

As it could be demonstrated during our tests, both the geometric accuracy of the self-calibrating AT as well as the image based generation of elevation data clearly profited from the tremendously increasing number of successful matches if digital cameras are used instead of scanned film. However, this matching accuracy and reliability is not only influenced by the respective sensor characteristics, but also by the atmospheric and illumination conditions during image flights.

This paper is the first English publication of the project but it only partially describes results from the geometric performance analysis and the automatic elevation model generation. Results from the radiometry and stereoplotting working groups are not given at all. More comprehensive papers will be compiled in near future. The most recent project progress is always documented on the project web site [DGPF, 2009], the next comprehensive project group meeting will take place as workshop in Stuttgart, October 5-6, 2009. Interesting people are cordially invited to participate in this workshop or any other project activity.

6. ACKNOWLEDGEMENTS

The authors would like to acknowledge all people involved in project preparation, data acquisition and/or data processing. Special thanks has to be expressed to Mr. Werner Schneider from ifp, who not only looks for all things regarding the Vaihingen/Enz test site but also is in charge for the data transfer between pilot centre and project participants. Thanks for support!

7. REFERENCES

Cramer, M., 2007: The EuroSDR performance test for digital aerial camera systems, in Fritsch (ed.): Photogrammetric Week 07, Wichmann, Heidelberg, p. 89-106, online available at http://www.ifp.uni-stuttgart.de/publications/phowo07/120Cramer.pdf, last access April 27, 2009.

Devencia, K., Walker, S. & Zhang, B. 2007: New Approaches to Generating and Processing High Resolution Elevation Data with Imagery. Photogrammetric Week, 17 (5), S. 1442-1448.

DGPF, 2009: project web site, www.ifp.uni-stuttgart.de/dgpf/ last access April 27, 2009.

Kraus, K., 2007: Photogrammetry, 2nd edition, de Gruyter, Berlin & New York, 459 p.

Lemaire, C., 2008: Aspects of the DSM Production with High Resolution Images IAPRS, Volume XXXVII, Part B4, S. 1143-1146.

Passini, R. & Jacobsen, K.: Accuracy analysis of large size digital aerial cameras, in Proceedings ISPRS Congress Beijing 2008, Volume XXXVII, Part B1, Commission I, WG I/4, p. 507-513.

Richter, R., 2009: ATCOR-4 User Guide, Version 5.0, available at http://www.rese.ch/pdf/atcor4_manual.pdf, last access April 27, 2009.

Schönermark, M. von, Kirchgäßner, U., Schwarzbach, M., Putze, U. & Dong Z., 2009: Überblick über die Arbeiten der Radiometriegruppe zur DGPF-Jahrestagung, online publication available at http://www.ifp.uni-stuttgart.de/dgpf/PDF/Jena09-Paper-Schoenermark-Radiometrieueberblick.pdf, last access April 27, 2009.

Klonus, S., Hagedorn, S., Jordan, E., Castillo, K., Gonzalo, J., Velez, F., 2009: Digitalisierung der Landnutzungserhebungen und erste Klassifikationsergebnisse, online publication available at http://www.ifp.uni-stuttgart.de/dgpf/PDF/JT09-Klonus_etal_statusreport.pdf, last access April 27, 2009.